Chinese Journal of Catalysis 36 (2015) 933–942

available at www.sciencedirect.com

ScienceDirect

journal homepage: www.elsevier.com/locate/chnjc

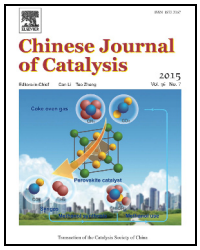

Article

Cr-free Co–Cu/SBA-15 catalysts for hydrogenation of biomass-derived α-, β-unsaturated aldehyde to alcohol

Sanjay Srivastava [a], Pravakar Mohanty [b,c], Jigisha K. Parikh [a,*], Ajay K. Dalai [d], S. S. Amritphale [e], Anup K. Khare [e]

[a] *Department of Chemical Engineering, S. V. National Institute of Technology, Ichchhanath, SURAT-395 007, Gujarat, India*
[b] *Department of Chemical Engineering, Indian Institute of Technology, New Delhi-110016, India*
[c] *Sardar Patel Renewable Energy Research Institute (SPRERI), V V Nagar, Gujarat 388120, India*
[d] *Catalysis and Chemical Reaction Engineering Laboratories, Department of Chemical and Biological Engineering, University of Saskatchewan, Saskatoon, Saskatchewan S7N 5A9, Canada*
[e] *Advanced Material and Processes Research Institute (AMPRI), Council of Scientific & Industrial Research (CSIR), Bhopal 462064, India*

ARTICLE INFO

Article history:
Received 13 January 2015
Accepted 21 April 2015
Published 20 July 2015

Keywords:
Mesoporous catalyst
Cobalt
Copper
SBA-15
Furfural
Furfuryl alcohol
Hydrogenation

ABSTRACT

Cr-free bi-metallic SBA-15-supported Co–Cu catalysts were examined in the conversion of biomass-derived α-, β-unsaturated aldehyde (furfural) to value-added chemical furfuryl alcohol (FOL). Co–Cu/SBA-15 catalysts with a fixed Cu loading of 10 wt% and varying Co loadings (2.5, 5, and 10 wt%) were prepared by the impregnation method. The catalysts were characterized by X-ray diffraction, N_2 sorption, H_2 temperature-programmed reduction, scanning electron microscopy, energy-dispersive X-ray spectroscopy, high-resolution transmission electron microscopy, CO chemisorption, and inductively coupled plasma mass spectrometry. The influence of different reaction parameters such as temperature, pressure, catalyst dosage, and furfural concentration on the catalyst performance was evaluated. Relative to catalysts supported on amorphous silica, the current SBA-15-supported Co–Cu catalysts displayed higher performance, attaining a furfural conversion of 99% and furfuryl alcohol selectivity of 80%. The catalytic reactions were conducted in a 100-mL autoclave at 170 °C and 2 MPa H_2 pressure for 4 h.

1. Introduction

Over the last few decades, interest in using biomass-derived molecules for conversion into fuels and chemicals has increased considerably owing to major concerns relating to global warming from anthropogenic emissions of greenhouse gases, climate change, and depletion of fossil fuel reserves [1]. However, biomass-derived molecules contain high oxygen contents. Thus, efficient and environmentally friendly catalysts have been investigated for selectively tailoring their oxygen content to achieve the desired products [2]. Furfural has been considered as a promising platform (as a building block) for the production of fuel and chemicals. Furfural is mainly produced by triple dehydration of sugar (xylose) in the presence of an acid catalyst [3–5]. Over the last two decades, the importance of hydrogenation of furfural (FFR) in the industrial context has grown because it can be successfully employed to synthesize a wide range of products such as furfuryl alcohol (FOL), 2-methyl furan (MF), tetrahydrofurfuryl alcohol (THFOL), tetrahydrofuran, and furan [6]. However, the selective hydrogenation of FFR to FOL has received the most interest because FOL has diverse applications such as in the manufacture of thermostatic resins,

* Corresponding author. Tel: +91-261-2251689; E-mail: jk_parikh@yahoo.co.in
DOI: 10.1016/S1872-2067(15)60870-1 | http://www.sciencedirect.com/science/journal/18722067 | Chin. J. Catal., Vol. 36, No. 7, July 2015

installation of acid-resistant bricks, and in anti-corrosion fiber glasses, resins (liquid) used in galvanic bath tub rubbers, and farm chemicals. FOL is also used as a non-reactive diluent for epoxy resin, a modifier for phenolic and urea resins, an oil well, and a carbon binder [7–12]. Furthermore, the salt of furfuryl alcohol is used in the synthesis of lysine, vitamin C, lubricants, and plasticizers.

Since the last five to six decades, bimetallic Cr–Cu catalysts have been widely used in the hydrogenation of FFR [13–15]. However, owing to the high toxicity and environmental concern of Cr–Cu alloys, research has focused on the development of alternative catalysts displaying higher yields and selectivity toward the hydrogenation of FFR [16–19]. As potential candidates, Co/Cu/Zn/Zr alloy [7], Raney Ni [20,21], Raney Co [22,23], Raney Cu [24], and various supported catalysts (Pd–Cu [25], Ni–Fe [26], Pt–Sn [27], Ni–Cu [28], Co–Cu [28], and Cu–Ca [29] supported on SiO_2, and CoB [30], CoMoB [31], NiMoB, and NiMo–B [32] supported on Al_2O_3) have been examined and applied by various groups of researchers. However, most of the reported catalysts are relatively expensive and provide moderate product selectivity at high reaction temperatures [28]. Amorphous silica-supported catalysts have also been considered for application in the hydrogenation of FFR to FOL (Table 1). However, their application is limited by their low FFR conversion and/or FOL selectivity.

Therefore, the goal of the present study was to develop a modified set of mesoporous silica-supported bi-metallic catalysts with high surface areas to achieve high conversions and good selectivity for FOL. SBA-15 is a hydrothermally stable mesoporous silica material featuring a large surface area and a highly ordered porous structure with uniform hexagonal channels with dimensions ranging from 5 to 30 nm [33]. It has been widely employed as a catalyst support owing to its advantageous features such as high surface-to-volume ratio and variable framework compositions. Its large pore size can lower the diffusion barrier for the reactants and products [33]. Furthermore, the strong interaction between Co and Cu affords enhanced dispersion and stability of Cu in the bi-metallic catalyst synthesis [28].

Table 1
Amorphous SiO_2-supported catalysts used in the hydrogenation of furfural.

Catalyst	t (°C)	p (bar)	Conversion (%)	FOL selectivity (%)	Ref.
Pd–Cu/SiO_2	250	1	50	16	[25]
Co–Cu-SiO_2	200	1	60	98	[28]
Co–Ni-SiO_2	200	1	10	82	[28]
Ni–Cu-SiO_2	200	1	32	96	[28]
1%Pd/SiO_2	230	1	69	10	[53]
10%Cu/SiO_2	230	1	69	68	[53]
5%Ni/SiO_2	230	1	100	19	[53]
Cu/SiO_2 (I)	110	10	4.8	0.8	[13]
Cu/SiO_2 (PD)	110	10	66.3	21.4	[13]
Cu–Ca/SiO_2	130	1	66	90	[29]
Pt/SiO_2	100	10	46	99	[52]
Ni/SiO_2	100	10	31	97	[52]
Ru/SiO_2	100	10	15	76	[52]
Ni–Fe/SiO_2	210	1	96	10	[26]

In the present study, Cr-free SBA-15-supported Co–Cu catalysts were prepared with varying loadings of Co (2, 5, and 10 wt%). Co was used as a promoter to Cu metal to enhance the activity and/or selectivity of the resulting catalysts by increasing the surface area or acting as a weak acid site to polarize the C=O bond in furfural [34]. The activity and selectivity of the prepared catalysts were assessed toward the hydrogenation of furfural. The catalytic performance of the SBA-15-supported catalysts was compared with that of amorphous silica-supported catalysts reported in the literature (Table 1). Furthermore, the effects of different operating parameters, such as reaction temperature, hydrogen pressure, catalyst dosage, and furfural concentration, on the catalytic performance were studied to optimize the furfural conversion and furfuryl alcohol selectivity.

2. Experimental

2.1. Materials

High purity (>99%) chemicals, tetraethyl orthosilicate (TEOS), pluronic (P123, $PEO_{20}PPO_{70}PEO_{20}$), $Co(NO_3)_2{\cdot}6H_2O$, $Cu(NO_3)_2{\cdot}6H_2O$, HCl (37%), and ethanol, were procured from Sigma-Aldrich (Mumbai, India), and demineralized water was used in this study.

2.2. Catalyst preparation

SBA-15 was synthesized as reported by Zhao et al. [33]. In a typical procedure, 4 g P123 was dissolved in 40 mL distilled water at 35 ± 1 °C for 2 h, whereby P123 acted as an organic template. Thereafter, 240 g HCl solution (2 mol/L) was added at 40 ± 1 °C, followed by the addition of 17.0 g TEOS with stirring. The mixture was stirred for 24 h at 40 ± 1 °C, then aged in a Teflon-coated polypropylene bottle at 100 ± 2 °C for 24 h. The final solid product was filtered, washed with deionized water, dried in the air, and calcined at 550 ± 4 °C under static conditions for 6 h, with a heating rate of 1.8 °C/min to remove the template agent.

Bi-metallic Co–Cu/SBA-15 catalysts were prepared by impregnation techniques reported in the literature [35] using salt solutions of $Co(NO_3)_2{\cdot}6H_2O$ and $Cu(NO_3)_2{\cdot}6H_2O$. The catalysts were dried for 12 h at 100 ± 2 °C and subsequently calcined at 450 ± 5 °C for 4 h to obtain the Cu–Co oxide catalysts. The Co–Cu/SBA-15 catalysts (Cu 10 wt%) with 10, 5, and 2.5 wt% of Co loadings are respectively denoted as CAT-A, CAT-B, and CAT-C.

2.3. Catalyst characterization

X-ray diffraction (XRD) patterns were obtained on a Philips PW-1710 X-ray diffractometer (Netherlands), equipped with Quasar software packages, using Cu K_α radiation produced from a PW Bragg–Brentano (BB) goniometer ($\theta/2\theta$), operating at 45 kV and 40 mA. The samples were scanned in the ranges of 2θ = 5°–80° and 2θ = 0.5°–10° for wide-angle and small-angle

XRD analyses, respectively.

The Brunauer–Emmett–Teller (BET) surface area, pore volume, and Barrett–Joyner–Halenda (BJH) (meso) pore size distribution of the prepared catalysts were determined by N_2 adsorption-desorption analysis conducted at −196 °C. Prior to analysis, the catalysts were degassed under vacuum at 200 ± 2 °C on an ASAP 2010 Micromeritics instrument.

The morphology of the catalysts was determined on an xT Nova NanoLab 200 field-emission scanning electron microscope (FESEM) equipped with an EDX unit. For analysis, the samples were sonicated in acetone (solvent) to disperse the sample uniformly. Thereafter, small drops of the sample were deposited on a carbon holder followed by evacuation under high vacuum (10^{-5} Torr). The samples were analyzed with an average of ten point analysis.

A Philips CM10-1990 transmission electron microscope (TEM) was used to further assess the morphology of SBA-15 and the prepared catalysts. For analysis, the powder catalyst material was dispersed in acetone using an ultrasonic bath for 15 min. A droplet of the suspended material was then placed on copper grids.

SEM-energy dispersive X-ray spectroscopy (SEM-EDX) was used to obtain rapid, qualitative, and some quantitative analysis of the elemental composition of the catalysts, with a sampling depth of 1–2 μm. The overall elemental molar composition of the prepared catalysts was confirmed by incluctively coupled plasma mass spectrometry (ICP-MS). In a typical procedure, 0.1 g catalyst was dissolved in concentrated HF acid (48%–51%) at 100–150 °C for 2 d. To ensure complete dissolution of the metals, concentrated HNO_3 was added, and the samples were examined on a mass spectrometer.

H_2 temperature-programmed reduction (TPR) analysis was carried out on a Micromeritics Pulse Chemisorption Chemisorb 2720 analyzer. In a typical procedure, 0.5 g catalyst was placed in a quartz reactor that was introduced into a furnace. The furnace temperature was increased from ambient to 800 °C, with a heating ramp of 10 °C/min. H_2 (9.9%) in Ar was used for reduction at a flow rate of 30 mL/min. H_2 consumption was measured using a thermal conductivity detector.

A Micromeritics ASAP 2020 Chemisorption system was used to measure the CO uptake on the oxide catalysts to calculate the metal surface area and dispersion. Prior to the experiment, the sample was subjected to vacuum and backfilled with He at 35 °C, and then evacuated at 110 °C for 60 min. The sample was then heated to 350 °C at 10 °C /min in the presence of H_2 and maintained at 350 °C for 2 h. The sample was then cooled to 35 °C and evacuated until the static pressure was less than (1.3–10.5) × 10^{-5} bar. The chemisorption analysis was performed by passing pulses of CO over the sample to measure the total CO uptake at 35 °C.

2.4. Catalytic activity

All reactions were performed at a laboratory scale using high pressure (SS-316) stirred autoclave of 100 mL capacity, supplied by Amar Equipment Pvt. Ltd. (Mumbai, India), equipped with an electrical heating jacket. Prior to reaction, the reactor was kept under N_2 pressure for the leak test. A known amount of catalyst was reduced by passing H_2 at 260 ± 2 °C. When the reactor was cooled to room temperature, furfural and isopropyl alcohol (molar ratio of 0.13) were charged into the reactor, which was flushed with N_2. The reactor was pressurized with H_2 (20 bar) and the reaction was carried out at 170 ± 1 °C. Each batch process experiment was subjected to thorough mixing at 1000 r/min [36]. The reproducibility of the experimental analysis was ensured by repeating each run three times; the reproducibility was within acceptable limits, thereby ensuring the absence of gas-liquid, liquid-solid, and intra-particle mass transfer limitations.

The product samples were analyzed on a Perkin Elmer Clarus 500 GC system equipped with a flame ionization detector. A Stabilwax capillary column with dimensions of 50 m × 0.25 mm × 0.5 μm was used. In a typical procedure, the initial oven temperature was maintained at 80 °C for 4 min and increased to 220 °C with a ramp of 20 °C/min, and subsequently maintained for 4 min. The product suspension (2 μL) in isopropanol was injected into the capillary column using a split ratio of 20:1 [7], whereby Ar was used as a carrier gas. The formation of furfuryl alcohol and other by-products were confirmed by gas chromatography–mass spectrometry. The following equations were used to determine the furfural conversion (X_{FFR}), product selectivity (S), and yield:

$$X_{FFR} = (\text{Initial moles of furfural} - \text{final moles of furfural})/\text{initial moles of furfural} \times 100\%$$

$$S = \text{Moles of desired product/moles of all products} \times 100\%$$

$$\text{Yield} = \text{Conversion (starting material)} \times \text{selectivity (desired product)} \times 100\%$$

3. Results and discussion

3.1. Synthesis and characterization

The small-angle XRD patterns of the SBA-15 support and CAT-A, CAT-B, and CAT-C catalysts are shown in Fig. 1. The spectra displayed well-resolved diffraction peaks at 2θ = 0.6°, 1.5°, and 1.7°, corresponding to (100), (110), and (200) diffraction planes. These could be indexed to the hexagonal unit cell reflections of SBA-15 [33], thereby confirming that the mesoporous structure was preserved following loading of Cu and Co [37–39]. However, the presence of Cu and Co on the support led to a decrease in the intensity of the lower angle diffraction peak (0.6°), which can be related to the scattering effects of the metallic Cu and Co particles.

Fig. 2 depicts the wide-angle XRD patterns of the SBA-15 support and CAT-A, CAT-B, and CAT-C catalysts. All three catalysts displayed sharp diffraction peaks at 2θ = 35.5° and 38.7°, corresponding to the planes (111) and (111) of monoclinic copper oxide (JCPDS 80-1917, 45-0937) [40,41].

This indicates the presence of large metallic crystallites in the Co–Cu/SBA-15 catalysts. The size of the CuO crystallite was 16–40 nm, as calculated by the Scherrer formula. Furthermore, the intensity of the diffraction peaks corresponding to the copper oxide crystallites decreased with increasing amounts of cobalt, owing to the good dispersion of the copper oxide parti-

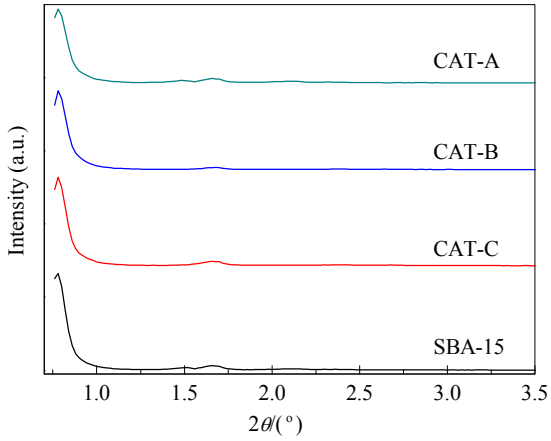

Fig. 1. Small-angle XRD patterns of SBA-15, CAT-A, CAT-B, and CAT-C.

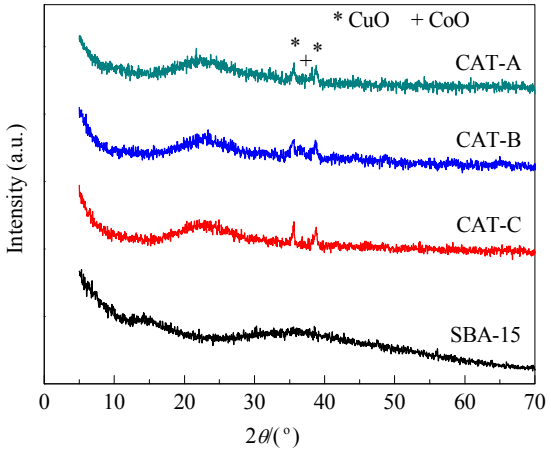

Fig. 2. Wide-angle XRD patterns of SBA-15, CAT-A, CAT-B, and CAT-C.

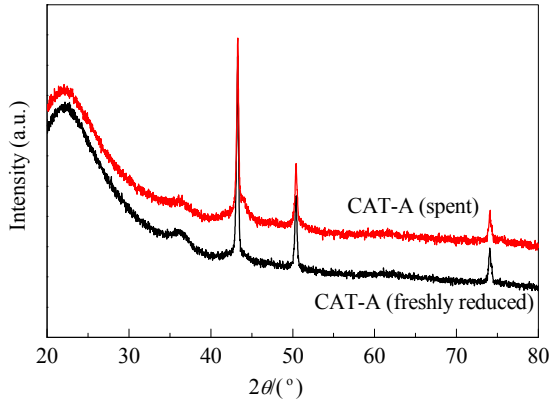

Fig. 3. Wide-angle XRD patterns of freshly reduced and spent CAT-A.

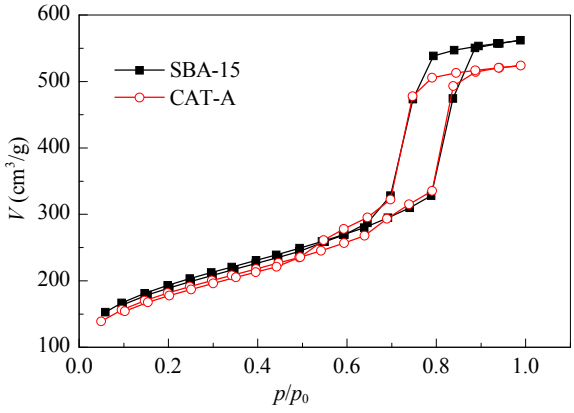

Fig. 4. N_2 adsorption-desorption isotherms of SBA-15 and CAT-A.

cles. These observations were supported by the BET surface area results, whereby the BET surface area of the catalysts increased with increasing cobalt loadings (Table 2). A weak diffraction at 2θ = 36.5°, corresponding to CoO, was also noted in CAT-B and CAT-A, whereby the loading contents of cobalt were high.

The presence of metallic copper (Cu^0) and cobalt (Co^0) on the surfaces of CAT-A (reduced and spent) could be deduced from the XRD patterns in Fig. 3. The characteristic diffraction lines of Cu^0, i.e., (111), (200), and (220) (*fcc* structure), were visible at 2θ = 43.6°, 50.8°, and 74.4°, respectively (JCPDS 04-0836). These findings were consistent with literature reports on Cu/SBA-15 [34]. In contrast, diffraction peaks corresponding to cobalt were absent.

The textural properties of the synthesized catalysts are summarized in Table 2. The SBA-15 support featured a BET surface area of 662 m^2/g and a total pore volume of 0.71 mL/g. As observed, the surface area of the bi-metallic catalysts increased with increasing amounts of Co. In contrast, the pore volume remained unchanged regardless of the Co loading content. This finding indicated that most of the metal particles were situated on the surface of SBA-15. These results further suggested that the loading of Co remarkably enhanced the dispersion of Cu and stability of Cu atoms on the support [28].

The N_2 adsorption-desorption isotherms of SBA-15 and CAT-A are presented in Fig. 4. Both samples displayed type IV isotherms with an H1 hysteresis loop. The shape of the isotherm of SBA-15 was preserved even after maximum loading of Cu and Co, indicating that the structural ordering of the parent material was preserved following incorporation of the metals. These results agreed with the small-angle XRD analysis.

Table 2
Textural and structural characteristics of support and its supported Cu–Co catalysts.

Sample	Cu:Co [a] (wt%)	Cu:Co [b] (wt%)	Cu:Co [c] (wt%)	S_{BET} (m^2/g)	V_p (mL/g)	D_p (nm)	d_p (nm)
SBA-15	—	—	—	661.6	0.71	7.7	—
CAT-A	10:10	10.45:10.11	10.90:9.30	405.5	0.55	5.6	42.75
CAT-B	10:5	9.15:5.23	9.46:4.52	362.9	0.53	5.4	54.45
CAT-C	10:2.5	8.92:2.12	9.32:2.04	342.0	0.50	5.2	72.55

[a] Loading ratio used in the synthesis.
[b] Evaluated by EDX analysis.
[c] Evaluated by ICP–MS analysis.

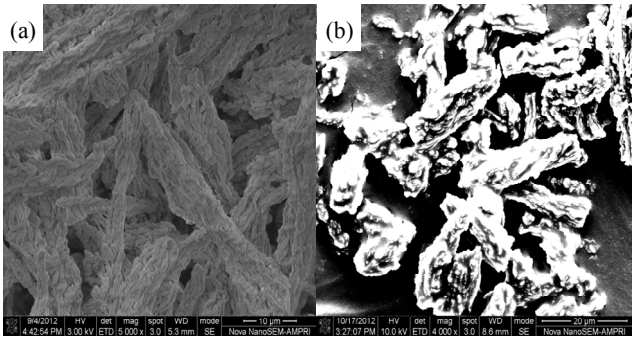

Fig. 5. FESEM images of SBA-15 (a) and CAT-A (b).

The FESEM images of SBA-15 and CAT-A are shown in Fig. 5. Large fibrous structures of 20–35 μm in length and 4–5 μm in diameter were observed for SBA-15. The fibrous structure is an agglomerate of long fibers that constitute small rod-like sub-particles [39]. Uniform distributions of the Cu and Co particles were observed with small agglomeration. To further evaluate the surface composition of the catalyst sample, EDX analysis was carried out. The results confirmed the presence of Co and Cu in appropriate proportions. The corresponding metal loadings are shown in Table 2. The results were, within acceptable errors, in accordance with the loading contents used in the synthesis process.

TEM analysis of SBA-15 (Fig. 6(a)) confirmed the presence of hexagonal arrays of uniform channels with a typical honeycomb morphology. Furthermore, the hexagonal symmetry of SBA-15 was retained following loading of the metal particles (Fig. 6(b) and (c)). Based on TEM analysis, the average particle size was calculated as 12–45 nm (Fig. 6(d)). These results were consistent with those from the XRD analysis.

The bulk elemental composition of the loaded catalysts was determined by ICP-MS and the results are shown in Table 2. The results were consistent with those obtained by EDX analysis and the loading contents used in the catalyst synthesis.

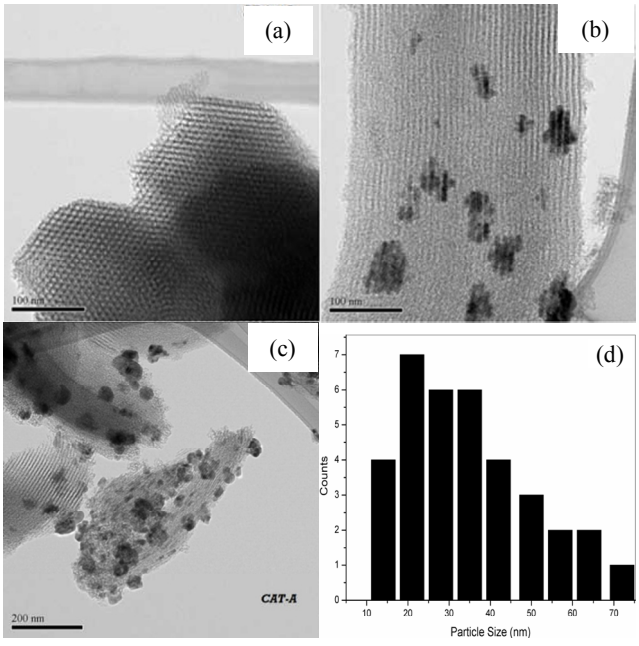

Fig. 6. HRTEM images of SBA-15 (a) and CAT-A (b, c). (d) Histogram of the size distribution of CAT-A particles.

H_2-TPR was used to determine the reducibility of the supported catalysts CAT-A, CAT-B, and CAT-C (Fig. 7). The bi-metallic samples displayed complex H_2-TPR profiles corresponding to several reduction steps. The peaks could be assigned to the reduction of CoO and CuO to partially reduced oxide species and ultimately to Cu and Co metal phases, as consistent with the XRD results.

Furthermore, the TPR profiles of the catalysts changed significantly with Co loading. This behavior may be attributed to the stepwise reduction of CuO and its level of interaction with Co. CAT-A, prepared at a Cu-to-Co ratio of 1, displayed a broad peak with two shoulders at 320–360 °C. In contrast, CAT-B, prepared at a higher Cu-to-Co ratio of 2, displayed peaks shifted to slightly higher temperatures. Further increasing the Cu-to-Co ratio to 4 generated three distinct peaks, which could be attributed to the formation of highly dispersed CuO and CoO at moderate temperatures and the formation of small Cu–Co clusters at higher temperatures above 400–440 °C [42,43].

During the TPR analysis, reduction of CuO can either follow a one-step $Cu^{2+} \rightarrow Cu^0$ mechanism or proceed through an intermediate Cu^+ state. The presence of an intermediate Cu^+ state depends on the conditions employed for the reduction process such as gas flow rate and temperature ramp. For all three catalysts tested, reduction proceeded via a two-step process because of the relatively slow ramp rate and gas flow rate selected for the TPR analysis. H_2 consumption by both CuO and CoO may have contributed proportionately to their available weight proportion to the reduction process as a result of spill-over effects [44]. Furthermore, Tien-Thao et al. [45] have suggested that copper provides active sites for higher alcohol synthesis to activate cobalt reduction and possibly modify cobalt by alloying. After reduction of the highly dispersed CuO, formation of small Cu^0 occurs in CAT-A (Fig. 3). Xu et al. [46] also reported that Cu–Co alloy was responsible for higher alcohol synthesis. Baker et al. [47] and Mohanty et al. [48] proposed that the active center comprised metallic Co atoms on Cu clusters and the active catalyst consisted of Cu particles supported on Co/Cr spinel.

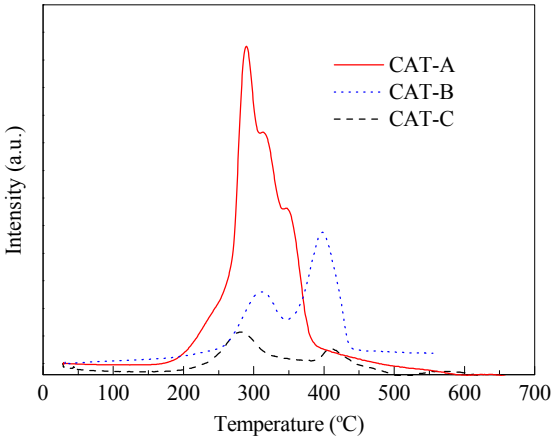

Fig. 7. H_2-TPR profiles of CAT-A, CAT-B, and CAT-C.

Table 3
CO chemisorption analysis of the catalysts.

Catalyst	Co (wt%)	Amount of adsorbed CO (μmol/g)	Metal dispersion (%)	Metal surface area (m^2/g of sample)	Metal crystallite size (nm)
CAT-A	10	1417.91	1.39	1.75	42.75
CAT-B	5	1000.74	1.14	1.32	54.45
CAT-C	2.5	809.98	1.01	1.10	72.55

CO chemisorption results of CAT-A, CAT-B, and CAT-C are presented in Table 3. It could be concluded that dispersion of Cu increased with increasing loadings of Co. The average metal crystallite size of CAT-A, as assessed by CO chemisorption, was 42.75 nm, which was consistent with the XRD and TEM results. The metal crystallite size increased with decreasing Co contents. Furthermore, the amount of CO adsorbed on the catalysts increased with increasing loadings of Co, thereby indicating that the dispersion of metallic copper was higher in CAT-A when compared with that in other catalysts. As observed, increasing the amount of Co increased the dispersion of Cu that is believed to promote catalyst activity and subsequent FOL selectivity.

3.2. Catalytic studies

All synthesized catalysts were examined in the hydrogenation of furfural in liquid phase using isopropanol as a solvent. Solvent effects in hydrogenation reactions over heterogeneous catalysts have been rationalized by correlating reaction rates and product distributions with solvent polarity and dielectric constant. The nature of the solvent can influence the kinetics of competitive hydrogenation reactions of both polar and non-polar substrates. It was observed that polar solvents enhance the adsorption of non-polar reactants, whereas non-polar solvents enhance the adsorption of polar reactants [7,27,34]. In the present work, we investigated the effect of isopropanol in the liquid-phase hydrogenation of furfural. As reported, this solvent is a suitable medium for the hydrogenation of furfural [7,27]. The stability of isopropanol was studied by reaction with hydrogen in the presence of CAT-A at 170 °C and 20 bar. The result showed that isopropanol was stable as it was fully recovered after 4 h of reaction. Additionally, the hydrogenation of furfural under solvent-free conditions was carried out for comparison. The results revealed that in the absence of isopropanol, a furfural conversion of 40.6% and a furfuryl alcohol yield of 62.7% were achieved. In contrast, in the presence of isopropanol, the conversion was 99% and the furfuryl alcohol selectivity was 80% (Table 4).

3.2.1. Efficacy of various catalysts

As mentioned previously, the hydrogenation of furfural can result in several byproducts, such as tetrahydrofurfural, THFOL, MF, and other C_4 products. The formation of the desired product, furfuryl alcohol, can be optimized by selection of appropriate catalysts and reaction conditions. Cu-based catalysts have been mostly employed for the conversion of furfural, owing to the preferential interaction of the surface with the carbonyl group over the furan ring [12]. In this work, furfuryl alcohol was obtained as the main product with small amounts of byproducts, MF and cyclopentanol (CPL), in the presence of the Cu-based bimetallic Co–Cu/SBA-15 catalysts. These results agreed with the literature reported to date on copper-based amorphous or supported catalysts [6,7,13,34].

The catalytic activities of the as-prepared supported bi-metallic Co-Cu/SBA-15 catalysts were evaluated toward the selective hydrogenation of furfural in liquid phase (Table 4), and compared with those of amorphous silica-supported catalysts (Table 1). As observed, the current mesoporous silica-supported bi-metallic Co–Cu catalysts featured favorable sites to attain higher conversion when compared with the amorphous silica-supported catalysts. Based on the physiochemical characterization and preliminary observations, it could be confirmed that the high surface area and ordered porous structure of SBA-15 provided a better platform to generate active sites for the reactants. Furthermore, the presence of Co, as a promoter, in the current bi-metallic catalyst system influenced the repartition of copper between easily reducible and barely reducible copper phases. This phenomenon may be the reason for the higher dispersion of the metallic sites on the surface of SBA-15 support and the minimal changes noted in the uniform hexagonal channels.

However, a significant decrease in the selectivity toward furfuryl alcohol was observed for the SBA-15-supported catalysts. In combination with the HRTEM analysis, it was observed that the metal particles were generally randomly distributed in both the pores and surface of the SBA-15 support that may act as active sites for the transformation of furfuryl alcohol to MF and CPL. Villaverde et al. [13] examined different Cr-free Cu-based catalysts, such as Cu/SiO_2, CuZnAl, and CuMgAl, toward the liquid-phase hydrogenation of furfural. Among all catalyst systems studied, CuMgAl was the most appropriate catalyst for such a process. In contrast, amorphous silica-supported catalysts, which contain active sites mostly on their surface, displayed high selectivity toward furfuryl alcohol. In the present case, the metal particles that reside in the meso-

Table 4
Catalytic performance (conversion X_{FFR} and selectivity S) of the catalysts.

Catalyst	X_{FFR} (%)	S_{FOL} (%)	S_{MF} (%)	S_{CPL} (%)
Cu/SBA-15	62.32	56.68	9.12	—
Co/SBA-15	37.65	77.37	8.17	0.86
CAT-A[a]	40.64	62.72	Trace	—
CAT-A	99.38	80.12	8.62	10.12
CAT-B	87.39	68.08	7.61	9.64
CAT-C	80.46	62.83	6.20	8.62

Reaction conditions: 170 °C, 20 bar, furfural-to-isopropanol molar ratio 1:7, catalyst 1 g, 4 h. [a] In the absence of isopropanol.

pores of SBA-15 act as active sites for the formation of intermediate furfuryl alcohol, thereby allowing the formation of byproducts such as MF, owing to restricted access.

To determine the role of individual and combined effects of Cu and Co in the liquid-phase hydrogenation of furfural, separate reactions were performed using either Cu or Co supported on SBA-15. As observed, both Cu and Co supported on SBA-15 displayed low conversions of furfural of nearly 62.3% and 37.6%, respectively, with moderate selectivity of FOL. In contrast, by introducing cobalt as a co-metal, the activity of the resulting bi-metallic catalysts increased (Table 4). Both the conversion and furfuryl alcohol selectivity increased with increasing Co loading; CAT-A (Cu, Co 10 wt%) displayed the highest conversion and selectivity values. This result can be attributed to the higher dispersion of the Cu active sites, as influenced by the presence of Co. In combination with the N_2 sorption and CO chemisorption analyses, it could be deduced that Co enhanced the dispersion of Cu; CAT-A displayed the highest surface area and metal dispersion. Additionally, based on the XRD analysis of reduced CAT-A (fresh and spent), only metallic Cu was present, which suggested that in the presence of Co, Cu was completely reduced. Thus, metallic Cu was responsible for the excellent catalytic behavior of the Co–Cu/SBA-15 catalysts. Furthermore, the TPR results indicated that reduction of CuO either followed the $Cu^{2+}\rightarrow Cu^0$ mechanism or proceeded through an intermediate Cu^+ state. Hence, it could be deduced that Co played an important role in the reduction of Cu. CAT-C and CAT-B (low Co contents of 2.5 and 5 wt%, respectively) displayed two broad peaks that suggested the presence of Cu^+ and Cu^0. The concentration of Cu^0 increased with increasing loading amounts of Co, as indicated by the increased intensity of the secondary peaks. In contrast, reduction seemed to follow a $Cu^{2+}\rightarrow Cu^0$ mechanism in the presence of CAT-A (higher Co content of 10 wt%), as consistent with the XRD analysis. It has been reported that in Co–Cu bimetallic catalyst systems, under O_2 conditions, both metals oxidize and Cu segregates from the surface as Cu^+. In contrast, under H_2 conditions, Co is reduced and Cu is fully reduced on the surface to Cu^0 [49]. In addition, Nagaraja et al. [50] proposed that the presence of more Cu^0 and Cu^+, as opposed to CuO, promoted high selectivity of furfuryl alcohol. Vargas-Hernandez et al. [34] reported a furfural conversion of 54% and FOL selectivity above 95% in the presence of 15 wt% Cu supported on SBA-15 at 170 °C. The high FOL selectivity was due to the presence of the more stable Cu^0 (Table 1). In this work, Co enhanced the dispersion of Cu particles and hence improved the overall conversion at a relatively low copper content of 10 wt%.

3.2.2. Optimization study

3.2.2.1. Effect of temperature

To examine the influence of temperature on the conversion of FFR (X_{FFR}) and selectivity of FOL (S_{FOL}), reactions were performed in the presence of CAT-A at varying temperatures within a range of 150–190 °C at a H_2 pressure (P_{H2}) of 20 bar.

As observed from Fig. 8, both X_{FFR} and S_{FOL} increased with increasing temperatures up to 170 °C, then decreased with further increases in temperature. Furthermore, the selectivity of MF increased at the expense of furfuryl alcohol. The substantial decrease in the selectivity of furfuryl alcohol may be attributed to further hydrogenolysis of FOL to MF at high temperatures that promotes C–O hydrogenolysis toward the cleavage of the carbonyl group. It is noteworthy that hydrogenation of furfural to FOL is dominant at low temperatures, whereas C–O hydrogenolysis is dominant at high temperatures owing to the higher activation of the latter process. Furthermore, the polymerization of FOL, owing to its adsorption onto the catalyst surface, is favored at high temperatures. These results agreed with literature reports [25,37,51]. Thus, a reaction temperature of 170 °C was employed in the subsequent experiments.

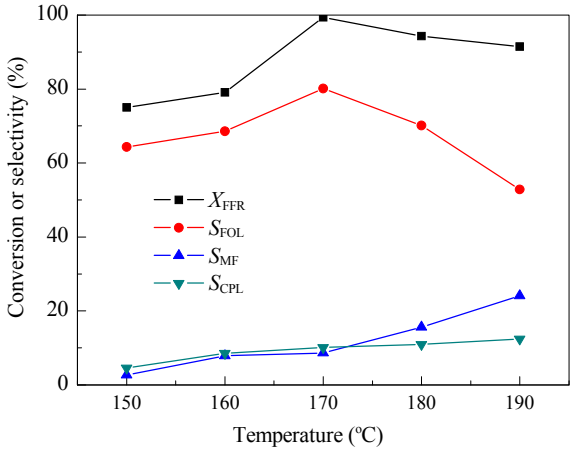

Fig. 8. Effect of temperature on the conversion of furfural to furfuryl alcohol using CAT-A. Reaction conditions: 20 bar, catalyst 1 g, 4 h, furfural-to-isopropanol molar ratio 1:7.

3.2.2.2. Effect of pressure

To optimize the H_2 pressure parameters, X_{FFR} and S_{FOL} were investigated in the presence of CAT-A at 170 °C and varying pressures of 10–40 bar. As observed, both the conversion and selectivity increased with increasing pressures up to 20 bar, after which no significant changes were noted (Fig. 9).

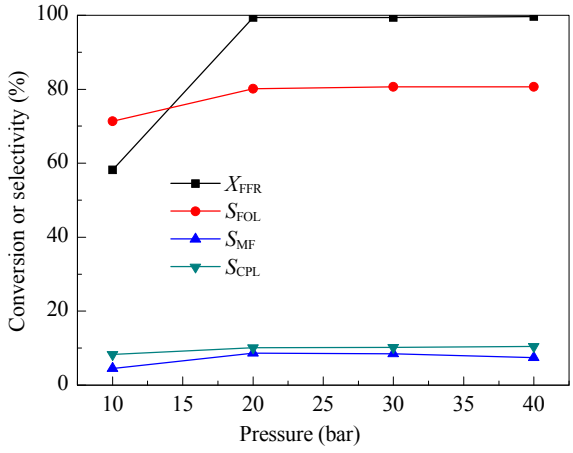

Fig. 9. Effect of H_2 pressure on the conversion of furfural to furfuryl alcohol using CAT-A. Reaction conditions: 170 °C, catalyst 1 g, 4 h, furfural-to-isopropanol molar ratio 1:7.

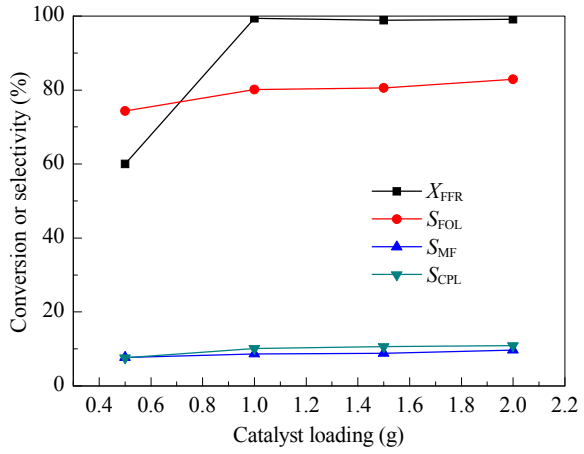

Fig. 10. Effect of catalyst dose on the conversion of furfural to furfuryl alcohol using CAT-A. Reaction conditions: 20 bar, 170 °C, 4 h, furfural-to-isopropanol molar ratio 1:7.

These observations were in agreement with the justifications as reported by Sharma et al. [7]. By increasing the pressure to 20 bar, the rate of reaction and conversion of furfural to furfuryl alcohol increased owing to the enhanced hydrogen solubility in the reaction mixture. At pressures above 20 bar, steady state conditions were attained. Therefore, a hydrogen pressure of 20 bar was chosen for the subsequent experiments.

3.2.2.3. Effect of catalyst dosage

The influence of catalyst dosage was investigated by increasing the catalyst weight from 0.5 to 2.0 g (Fig. 10). As observed, X_{FFR} and S_{FOL} increased with increasing catalyst dosages owing to the availability of more active sites. The highest conversion and selectivity were observed using 1 g of catalyst. Further increases in the catalyst dosage resulted in minimal changes. However, using higher catalyst dosages of 1.5 and 2.0 g resulted in faster reactions when compared with the reaction rate obtained in the presence of 1.0 g catalyst. Accordingly, a catalyst dosage of 1.0 g was considered in the subsequent studies.

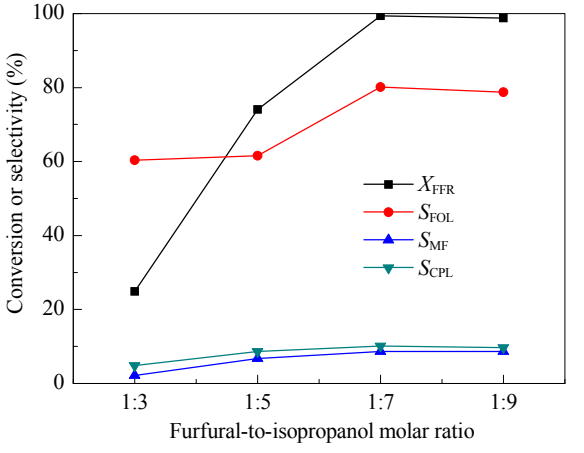

Fig. 11. Effect of furfural-to-isopropanol molar ratio on the conversion of furfural to furfuryl alcohol using CAT-A. Reaction conditions: 20 bar, 170 °C, 4 h, catalyst 1 g.

Table 5
Catalytic cyclic performance of CAT-A toward hydrogenation of furfural.

Catalyst	X_{FFR} (%)	S_{FOL} (%)	S_{MF} (%)	S_{CPL} (%)
CAT-A (fresh)	99.38	80.12	8.62	10.12
CAT-A (1st cycle)	95.46	79.48	8.46	9.65
CAT-A (2nd cycle)	94.26	79.24	8.82	9.78

Reaction conditions: 170 °C, 20 bar, furfural-to-isopropanol molar ratio 1:7, catalyst 1 g, 4 h.

3.2.2.4. Effect of furfural-to-solvent molar ratio

The furfural-to-solvent ratio was varied from 1:3 to 1:9 to examine its effect on the catalytic process in the presence of CAT-A (Fig. 11). As observed, both X_{FFR} and S_{FOL} decreased with increasing furfural concentrations owing to the availability of fewer active sites to convert furfural to furfuryl alcohol. This finding revealed that higher yields could be obtained at low furfural concentrations (i.e., high molar ratios). Moreover, high furfural concentrations are often detrimental to the stability of active sites on the catalyst surface, thereby reducing the rate of hydrogenation. As reported, high furfural concentrations in liquid-phase hydrogenation of furfural do not favor overall conversion or selectivity of the desired products [13]. Accordingly, a molar ratio of 1:7 was employed in the subsequent studies.

3.2.3. Stability of catalyst in the hydrogenation of furfural

CAT-A catalyst that exhibited the best catalytic efficiency was recycled twice to evaluate its stability. Owing to possible carbon deposits from the organic reactants or products on the surface of the catalyst during the catalytic reactions, a reaction temperature of 500 °C was used for calcination to remove potentially adsorbed or deposited carbon species. XRD was employed to monitor structural changes in the spent and the freshly reduced catalysts. The XRD patterns are shown in Fig. 3. As expected, similarly to the freshly reduced CAT-A, most stable Cu^0 species were detected in the spent CAT-A catalyst, as indicated by the diffraction peaks at 2θ = 43.6°, 50.8°, and 74.4°, which were respectively indexed as (111), (200), and (220) (*fcc* structure) [14]. The catalytic cyclic performance of CAT-A is presented in Table 5. A slight decrease in the conversion of FFR (nearly 5%) was observed. However, no changes in the selectivity of the desired product (FOL) were observed. Hence, the catalyst was stable for liquid-phase hydrogenation of furfural.

4. Conclusions

A series of bi-metallic Co–Cu catalysts supported on SBA-15, with a fixed Cu loading and varying Co loadings, were synthesized by the impregnation method. These catalysts were examined in the hydrogenation of furfural and compared with amorphous silica-supported catalyst counterparts. The results showed that the SBA-15-supported catalysts achieved higher conversions with considerable improvements in the selectivity of furfuryl alcohol when compared with literature-reported catalysts supported on amorphous silica. Furthermore, it was concluded that the selective structure of the mesoporous silica

Graphical Abstract

Chin. J. Catal., 2015, 36: 933–942 doi: 10.1016/S1872-2067(15)60870-1

Cr-free Co–Cu/SBA-15 catalysts for hydrogenation of biomass-derived α-, β-unsaturated aldehyde to alcohol

Sanjay Srivastava, Pravakar Mohanty, Jigisha K. Parikh *,
Ajay K. Dalai, S. S. Amritphale, Anup K. Khare
S. V. National Institute of Technology, India;
Indian Institute of Technology, India;
Sardar Patel Renewable Energy Research Institute (SPRERI), India;
University of Saskatchewan, Saskatoon, Saskatchewan, Canada;
Council of Scientific & Industrial Research (CSIR), India

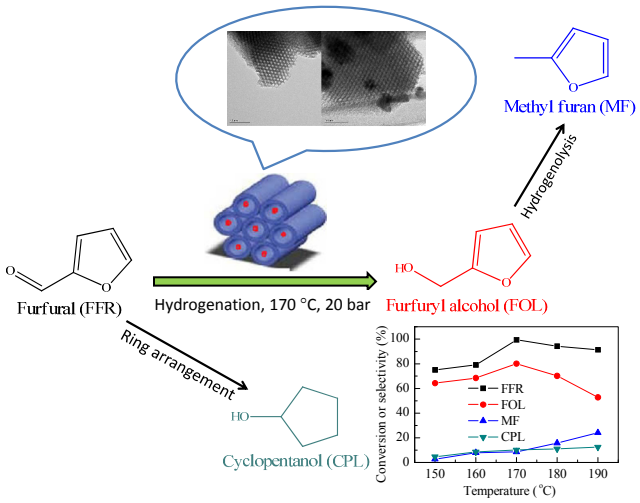

This work presents the hydrogenation of furfural in liquid phase, as a direct step for bio-oil upgradation, using bi-metallic Co–Cu catalysts supported on SBA-15 (Cu 10 wt%; Co 2.5, 5, 10 wt%).

network favored C–O hydrogenolysis and furan ring arrangement, generating 2-methyl furan and cyclopentanol. The presence of Co played an important role as a promoter in the hydrogenation activity by improving the dispersion of the Cu active sites. Co–Cu/SBA-15 (Cu 10 wt%, Co 10 wt%) attained a conversion of 99% and furfuryl alcohol selectivity of 80% at 170 °C, 20 bar H_2 pressure, using a catalyst dosage of 1 g and furfural-to-isopropanol molar ratio of 1:7.

References

[1] Corma A, Iborra S, Velty A. *Chem Rev*, 2007, 107: 2411
[2] Nanda S, Mohanty P, Pant K K, Naik S, Kozinski J A, Dalai A K. *Bioenergy Res,* 2013, 6: 663
[3] Butler E, Devlin G, Meier D, McDonnell K. *Renew Sustain Energy Rev*, 2011, 15: 4171
[4] Chiaramonti D, Oasmaa A, Solantausta Y. *Renew Sustain Energy Rev,* 2007, 11: 1056
[5] Yan K, Wu G S, Lafleur T, Jarvis C. *Renew Sustain Energy Rev,* 2014, 38: 663
[6] Yang W, Sen A. *ChemSusChem*, 2011, 4: 349
[7] Sharma R V, Das U, Sammynaiken R, Dalai A K. *Appl Catal A*, 2013, 454: 127
[8] Borts M S, Gilchenok N D, Ignatev V M, Gurevich G S. *J Appl Chem USSR,* 1986, 59: 114
[9] Rao R, Dandekar A, Baker R T K, Vannice M A. *J Catal,* 1997, 171: 406
[10] Vaidya P D, Mahajani V V. *Ind Eng Chem Res,* 2003, 42: 3881
[11] Rojas H, Martines J J, Reyes P. *Dyna,* 2010, 163: 151
[12] Sitthisa S, Sooknoi T, Ma Y, Balbuena P B, Resasco D E. *J Catal,* 2011, 277: 1
[13] Villaverde M M, Bertero N M, Garetto T F, Marchi A J. *Catal Today,* 2013, 213: 87
[14] Yan K, Chen A C. *Energy,* 2013, 58: 357
[15] Seo G, Chon H. *J Catal,* 1981, 67: 424
[16] Lee J Y, Lee D W, Lee K Y, Wang Y. *Catal Today,* 2009, 146: 260
[17] Yan K, Chen A C. *Fuel,* 2014, 115: 101
[18] Burnette L W, Johns I B, Holdren R F, Hixon R M. *Ind Eng Chem*, 1948, 40: 502
[19] Dong F, Zhu Y L, Zheng H Y, Zhu Y F, Li X Q, Li Y W. *J Mol Catal A*, 2015, 398: 140
[20] Liu B J, Lu L H, Wang B C, Cai T X, Katsuyoshi I. *Appl Catal A,* 1998, 171: 117
[21] Thomas D D. US Patent 4146460. 1979
[22] Erzhanova M S, Beisekov T B. SU Patent 450585. 1974
[23] Beisekov T B, Masaeva S A, Kuatbekov A M, Pilipenko S V, Utebaeva A. *Khim Promst,* 1992: 507
[24] Pljusnin L D, Beisekov T, Jerzhanova M S, Daurenbekov B D. *Khim Promst,* 1988: 672
[25] Sitthisa S, Pham T, Prasomsri T, Sookni T, Mallinson R G, Resasco D E. *J Catal,* 2011, 280: 17
[26] Sitthisa S, An W, Resasco D E. *J Catal,* 2011, 284: 90
[27] Merlo A B, Vetere V, Ruggera J F, Casella M L. *Catal Commun,* 2009, 10: 1665
[28] Reddy B M, Reddy G K, Rao K N, Khan A, Ganesh I. *J Mol Catal A,* 2007, 265: 276
[29] Wu J, Shen Y M, Liu C H, Wang H B, Geng C J, Zhang Z X. *Catal Commum,* 2005, 6: 633
[30] Li H, Chai W M, Luo H S, Li H X. *Chin J Chem,* 2006, 24: 1704
[31] Chen X F, Li H X, Luo H S, Qiao M H. *Appl Catal A,* 2002, 233: 13
[32] Wei S Q, Cui H Y, Wang J H, Zhuo S P, Yi W M, Wang L H, Li Z H. *Particuology,* 2011, 9: 69
[33] Zhao D Y, Feng J L, Huo Q S, Melosh N, Fredrickson G H, Chmelka B F, Stucky G D. *Science,* 1998, 279: 548
[34] Vargas-Hernandez D, Rubio-Caballero J M, Santamarıa-Gonzalez J, Moreno-Tost R, Merida-Robles J M, Perez-Cruz M A, Jimenez-Lopez A, Hernandez-Huesca A, Maireles-Torres. *J Mol Catal A,* 2014, 383-384: 106
[35] Yan K, Lafleur T, Jarvis C, Wu G S. *J Clean Prod*, 2014, 72: 230
[36] Ramachandran P A, Chaudhari R V. Three-Phase Catalytic Reactors. New York: Gordon and Breach, 1983. 427
[37] Klimova T, Reyes J, Gutierrez O, Lizama L. *Appl Catal A*, 2008, 335: 159
[38] Soni K, Mouli K C, Dalai A K, Adjaye J. *Catal Lett,* 2010, 136: 116
[39] Dhar G M, Kumaran G M, Kumar M, Rawat K S, Sharma L D, Raju B

D, Rama Rao K S. *Catal Today,* 2005, 99: 309
[40] Carrero A, Calles J A, Vizcaíno A J. *Appl Catal A,* 2007, 327: 82
[41] Zhu Y Y, Wang S R, Zhu L J, Ge X L, Li X B, Luo Z Y. *Catal Lett,* 2010, 135: 275
[42] Marchi A J, Di Cosimo J I, Apesteguia C R. *Catal Today,* 1992, 15: 383
[43] Cesar D V, Perez C A, Salim V M M, Schmal M. *Appl Catal A*, 1999, 176: 205
[44] Iglesia E, Soled S L, Baumgartner J E, Reyes S C. *J Catal,* 1995, 153: 108
[45] Tien-Thao N, Zahedi-Niaki M H, Alamdari H, Kaliaguine S. *J Catal,* 2007, 245: 348
[46] Xu X D, Mausbeck D, Scholten J J F. *Catal Today,* 1991, 10: 429
[47] Baker J E, Burch R, Hibble S J, Loader P K. *Appl Catal*, 1990, 65: 281
[48] Mohanty P, Pant K K, Parikh J, Sharma D K. *Fuel Process Technol,* 2011, 92: 600
[49] An K, Somorjai G A. *Catal Lett,* 2015, 145: 233
[50] Nagaraja B M, Siva Kumar V, Shasikala V, Padmasri A H, Sreedhar B, Raju B D, Rama Rao K S. *Catal Commun*, 2003, 4: 287
[51] Liu D X, Zemlyanov D, Wu T P, Lobo-Lapidus R J, Dumesic J A, Miller J T, Marshall C L. *J Catal,* 2013, 299: 336
[52] Vetere V, Merlo A B, Ruggera J F, Casella M L. *J Braz Chem Soc,* 2010, 21: 914
[53] Sitthisa S, Resasco D E. *Catal Lett,* 2011, 141: 784